

# Characterizing GPU Resilience and Impact on AI/HPC Systems

Shengkun Cui\*  
UIUC  
Urbana, IL, USA

Archit Patke\*  
UIUC  
Urbana, IL, USA

Ziheng Chen\*  
UIUC  
Urbana, IL, USA

Aditya Ranjan\*  
UIUC  
Urbana, IL, USA

Hung Nguyen  
UIUC  
Urbana, IL, USA

Phuong Cao  
UIUC  
Urbana, IL, USA

Saurabh Jha  
IBM Research  
Yorktown Heights, NY, USA

Brett Bode  
NCSA, UIUC  
Urbana, IL, USA

Gregory Bauer  
NCSA, UIUC  
Urbana, IL, USA

Chandra Narayanaswami  
IBM Research  
Yorktown Heights, NY, USA

Daby Sow  
IBM Research  
Yorktown Heights, NY, USA

Catello Di Martino  
Nokia Bell Labs  
Sao Paulo, Brazil

Zbigniew T. Kalbarczyk  
UIUC  
Urbana, IL, USA

Ravishankar K. Iyer  
UIUC  
Urbana, IL, USA

## Abstract

In this study, we characterize GPU failures in *Delta*<sup>1</sup>, the current large-scale AI system with over 600 petaflops of peak compute throughput. The system comprises GPU and non-GPU nodes with modern AI accelerators, such as NVIDIA A40, A100, and H100 GPUs. The study uses two and a half years of data on GPU errors. We evaluate the resilience of GPU hardware components to determine the vulnerability of different GPU components to failure and their impact on the GPU and node availability. We measure the key propagation paths in GPU hardware, GPU interconnect (NVLink), and GPU memory. Finally, we evaluate the impact of the observed GPU errors on user jobs. Our key findings are: (i) Contrary to common beliefs, GPU memory is over 30× more reliable than GPU hardware in terms of MTBE (mean time between errors). (ii) The newly introduced GSP (GPU System Processor) is the most vulnerable GPU hardware component. (iii) NVLink errors did not always lead to user job failure, and we attribute it to the underlying error detection and retry mechanisms employed. (iv) We show multiple examples of hardware errors originating from one of the key GPU hardware components, leading to application failure. (v) We project the impact of GPU node availability on larger scales with emulation and find that significant overprovisioning between 5–20% would be necessary to handle GPU failures. If GPU availability were improved to 99.9%, the overprovisioning would be reduced by 4×.

## Keywords

Measurements, Dependability Analysis, GPU Resilience, AI/HPC System, Field Data Study

<sup>1</sup>*Delta* is an NCSA operated high-performance computing system at University of Illinois Urbana-Champaign.

\*Equal Contribution.

## 1 Introduction

**Background and Objective.** Large-scale HPC systems are important not only for scientific workloads [49] but also for data analytics [1] and machine learning (ML) [21]. The main components of these systems are specialized accelerators, such as GPUs, that enable acceleration of computations, such as ML training [51, 54], ML inference [25], and simulations [39, 48].

This paper presents the results of a resilience study of *Delta* consisting of 1,168 NVIDIA GPUs: A40, A100, and H100 GPUs. The study uses two and a half years of data on critical GPU errors collected across the stated GPUs. In this study, we assess: (a) the resilience of GPU hardware components to identify the vulnerability of various GPU components to errors and their impact on GPU node availability, (b) the key error propagation paths in GPU hardware, GPU interconnect (NVLink), and GPU memory, and (c) the impact of the observed GPU errors on user jobs. Our study uncovers new failure paths such as the one shown in Figure 1. A GSP (GPU System Processor) error stalled GPU control functions and required node draining<sup>2</sup> of the node and a full node reboot was required to recover. The entire process took 23 hours.

**Key Findings.** Our major findings include:

(i) *Contrary to common beliefs, GPU memory is over 30× more reliable in terms of MTBE (Mean Time Between Errors) than GPU hardware.* Among the GPU hardware components, the newly introduced GSP (GPU System Processor), intended as a performance enhancer for offloading critical CPU driver tasks, is the most vulnerable due to its lack of robust detection and recovery. Our analysis shows that over 99% of GSP errors put the GPU in an error state, leading to user job failures. A GSP error requires a node reboot.

(ii) *Communication errors with PMU (Power Management Unit) can lead to issues such as the inability to change the GPU core clock*

<sup>2</sup>Node draining refers to the process of allowing existing jobs on a node to complete while preventing new jobs from being scheduled on it to prepare for node maintenance.

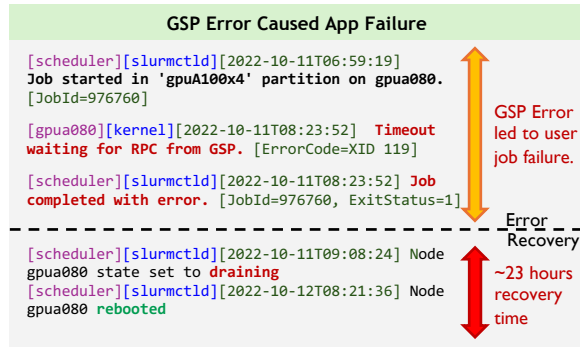


**Figure 1:** A GSP (GPU System Processor) error stalled GPU control functions and rendered the GPU inoperable (line 2). Consequently, the user job scheduled on that GPU failed, as reflected in the scheduler logs (line 3). The GSP error required draining the node and a full node reboot to recover, which led to the draining of all pending user jobs on that node (line 4). From the beginning of node drain to the completion of node reboot (line 5), the total recovery time was 23 node hours for this incident, during which the node was unavailable. This incident shows that a GPU error can significantly interrupt user jobs and node availability.

*frequency and memory clock frequency.* Propagation of such errors has an 82% chance of causing MMU (Memory Management Unit) errors, leading to a user job failure (97% chance).

(iii) *NVLink (GPU-to-GPU communication fabric within a multi-GPU node) errors occur with an MTBE of 6.9 hours system-wide.* Once encountered, an NVLink error has a 66% chance of leading to job failure. For the remaining 34%, the job that encountered an NVLink error completed successfully. We attribute this to error detection mechanisms such as CRC (cyclic redundancy check) that detect errors and trigger message retransmission to recover from communication errors.

(iv) *Newly introduced GPU memory error-recovery mechanisms on Ampere GPUs (e.g., memory row remapping, error containment) improve GPU memory resilience and reduce service interruption.* Our analysis shows that these mechanisms mitigate the impact of a DBE on applications by 70.6% of the time. However, failure in error containment can result in bursty and persistent memory errors (e.g., we encountered a case of an uncontained memory error that persisted for 17 days during testing period due to lack of monitoring to trigger a timely GPU reset), presenting a resilience challenge.

(v) *Hardware errors and lack of robust recovery in hardware lead to job failures.* Except for MMU and NVLink errors, none of the other hardware errors can be handled by application-level mechanisms. Hence, the reliability of the underlying GPU hardware needs to be improved, as relying on application-based recovery strategies is not feasible.

(vi) *The overall availability per GPU node is 99.5%, which corresponds to a downtime of 7 minutes per day.* Such a large downtime indicates that the infrastructure is not ready yet to meet the demands of critical applications that need to provide uninterrupted service. Additionally, we project the impact of this availability distribution on larger scales with emulation and find that significant overprovisioning between 5–20% would be necessary to handle

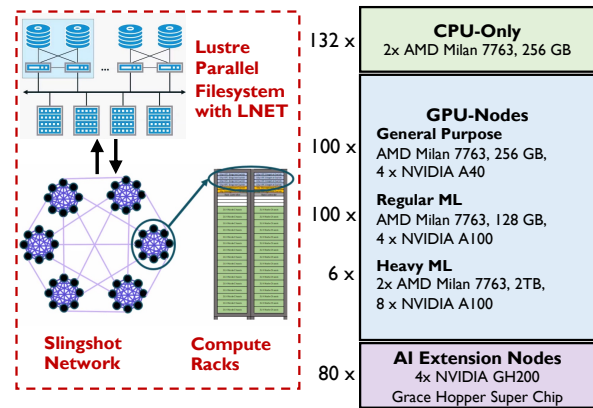


**Figure 2:** System architecture and specifications of *Delta*.

associated failures. While at first glance such overprovisioning may appear to be a small cost, for the example used in our study it would cost over 1 millions dollars per month. If GPU availability were improved to 99.9%, the overprovisioning would reduce by 4x.

**Putting the paper in perspective.** Previous studies on characterizing GPU resilience in large-scale systems [8, 9, 15, 16, 30, 31, 36, 37, 52, 53] focus on GPU memory errors in older GPU generations (Tesla, Kepler, and Volta) that lacks the latest resilience (e.g., row remapping, error containment, NVLink CRC-retry) and performance features (e.g., GPU System Processor) introduced in NVIDIA Ampere generation GPUs. To the best of our knowledge, this is the first study of GPU errors of the current (Ampere and Hopper) generation of NVIDIA GPUs on their memory, peripheral hardware, and NVLink components, and to derive error propagation models from real-world data using a generalizable methodology. The error propagation models help uncover resilience weak links (e.g., GSP and PMU) for the latest generation of GPU, driving GPU designs and system operational improvements, and enable error prediction and failure prevention for future research. The revealed GPU resilience weak links in our analysis are applicable to other HPC systems equipped with similar NVIDIA GPUs.

Broadly, resilience characterization studies analyze operational data on errors to provide insights into system reliability [8, 9, 15, 16, 30, 31, 36, 37, 52, 53]. While in those studies, the error rate is used as the key metric to quantify reliability, some [3, 50] argue that fault analysis is more appropriate. Although a fault may result in multiple errors, it is the resulting errors that the recovery mechanisms must address to maintain system health. Thus, in the longer term, knowing the underlying fault is valuable for building better systems. However at runtime, the system needs to handle the errors regardless of whether the underlying fault is permanent or transient [44]. Hence, like many others who study operational data, we chose to study errors.

## 2 Background

This section provides information on (i) *Delta* specification, (ii) critical GPU error categories used in this study, (iii) GPU error management and recovery, and (iv) *Delta* GPU utilization distributions.

## 2.1 Delta Specifications

*Delta* (Figure 2) is an AI system equipped with 132 CPU-only nodes and 286 GPU-accelerated nodes, designed to run diverse scientific research and artificial intelligence (AI)/machine learning (ML) workloads.

The *CPU-only* nodes are equipped with two 64-core AMD EPYC Milan CPUs. The *GPU-accelerated* nodes comprise four configurations of NVIDIA GPUs: (i) 4-way A40 (400 GPUs), (ii) 4-way A100 (400 GPUs), (iii) 8-way A100 (48 GPUs), and (iv) GH200 Gracehopper Super-chip (Arm64-based CPU and an recently released H100 GPU, 320 GPUs), a total of 1,168 current generation GPUs. A40 GPUs are intended for GPGPU and lightweight AI/ML applications. A100 and H100 GPUs, equipped with High Bandwidth Memory (HBM), are designed for demanding ML and HPC workloads. *Delta* is equipped with HPE Cray Slingshot 11 network that offers 400Gbps+ connectivity bandwidth between nodes, and Lustre file system for storage [4].

## 2.2 NVIDIA GPU Error Categories

NVIDIA GPU errors are reported as XID errors. In this study, we select a subset of XID errors that are described as common and high-impact by the NVIDIA’s Developer Manuals [32, 34], NVIDIA Developer Forums and Blogs, and *Delta* site reliability engineers (SREs). We primarily collect error-related events and their associated recovery events. The selected XID events indicate GPU hardware and driver issues that often cannot be resolved without SRE’s intervention. The selected XIDs and their corresponding GPU errors are described in Section 4, Table 1. We categorize the selected GPU errors into three categories: (i) GPU hardware, (ii) NVLink interconnect, and (iii) GPU memory.

General GPU Software Error (XID 13) and Reset Channel Verification Error (XID 43) are usually caused by user jobs and do not impact the health of the GPU [34]; we exclude those errors in our study.

**GPU Hardware Errors.** The critical GPU hardware errors we studied include MMU<sup>3</sup> errors, GPU Fallen Off the Bus errors, GSP<sup>4</sup> RPC timeout errors, and PMU<sup>5</sup> communication errors. We do not observe other GPU hardware errors in our study. GPU hardware errors can lead to user job failures, GPU halt, and data corruption. Among those errors, GPU Fallen Off the Bus and GSP RPC timeout errors lead to GPU failures, and manual GPU resets or node reboots are required to recover from the error [34]. *Delta* SREs monitor GSP RPC timeout errors closely to ensure timely recovery and maintain GPU availability.

**GPU Interconnect (NVLink) Errors.** GPU-GPU NVLink errors are caused by faulty GPU hardware, connectors, or improper installation during system integration and can lead to GPU unavailability and user job failures. Moreover, these errors impede data transfer between GPUs and reduce computational throughput. GPU reset or node reboot is required to clear NVLink errors [34].

<sup>3</sup>Memory management unit provides essential memory I/O functionalities.

<sup>4</sup>GPU system processor (GSP) is a co-processor on-board that offloads driver tasks from CPU for latency and performance improvement.

<sup>5</sup>PMU regulates the frequency, voltage, and power of the GPU based on various factors such as temperature and power cap, also referred to as the “Performance Monitoring Unit” by NVIDIA.

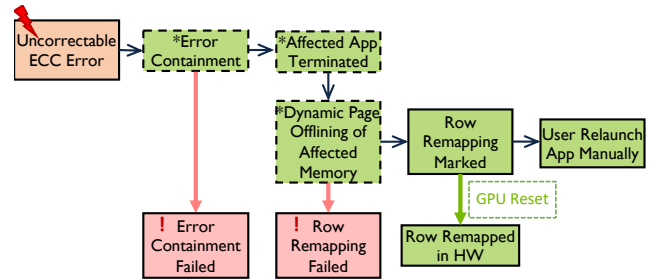


**Figure 3: NVIDIA memory error recovery process for A40, A100, and H100 GPUs. Error Containment and Dynamic Page Offlining are available on NVIDIA A100 and H100 only.**

**GPU Memory Errors.** GPU memory errors included in this study are double-bit errors (DBEs). Single-bit errors (SBEs) are not logged as they are automatically corrected by ECC. DBE triggers downstream error recovery mechanisms, which are introduced in Section 2.3. Failures in these mechanisms can lead to GPU/node failure and require GPU or node reboot to recover [34]. Although DBEs are rare, *Delta* SREs continuously monitor DBEs for timely replacement of faulty GPUs.

## 2.3 NVIDIA GPU Error Management

This section introduces the resilience architectures of NVIDIA A40, A100, and H100 GPUs.

### 2.3.1 Common Resilience Architecture.

**GPU Hardware.** While the GPU caches and memory are SECDED protected, information on failure-recovery mechanisms on GPU hardware, including peripheral hardware such as GSP, PMU, or SPI communication channels is limited.

**GPU Interconnect (NVLink).** NVLink employs Cyclic Redundancy Checks (CRCs) to ensure integrity of flow control digits and data. NVLink retries packet transmissions from the last-known good packet upon encountering a CRC checksum error.

**GPU Memory.** Figure 3 shows the error-recovery process for A40, A100, and H100, in more details. The primary mechanism to mitigate DBE for Ampere and Hopper GPUs is *row-remapping process*, which replaces the faulty memory row with a spare row, and a row-remapping event (RRE) is logged. If there is no available spares for that memory row, a row remapping failure (RRF) is indicated [32, 34]. Row-remapping failure (RRF) is logged when RRE fails as all available spare rows for that memory bank are exhausted [32, 34]. Additional error-recovery mechanisms like error containment and dynamic page offlining are discussed below.

### 2.3.2 Additional Resilience Features of A100 and H100.

Dashed-boxes in Figure 3 show additional recovery mechanisms for A100 and H100. A100 and H100 GPUs, compared to A40, supports uncorrectable memory error containment and dynamic page offlining [32, 34] for memory error mitigation. The dynamic page offlining marks the bad memory address as unusable without the need for a GPU reset to maintain availability. Error containment terminates user processes using the faulty memory address to prevent error propagation. Successful Error containment is logged as a

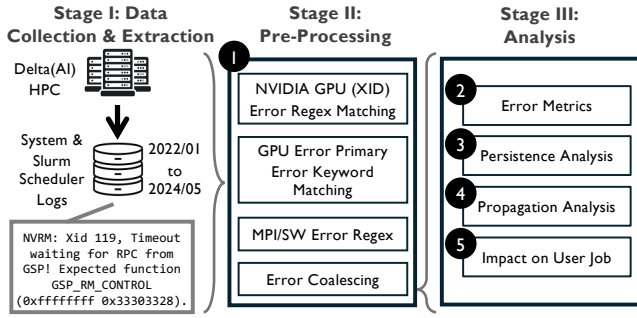


Figure 4: Overview of our data collection, processing, and analysis pipeline.

Contained Memory Error; whereas unsuccessful error containment is logged as an Uncontained Memory Error.

Failure in a row-remapping or error containment can cause a GPU failure that requires a GPU reset/node reboot to recover. *Delta* SREs monitor row-remapping failures and replace GPUs that repeatedly emit such errors.

## 2.4 *Delta* GPU Utilization

*Delta*'s NVIDIA Ampere GPUs, A100 and A40 GPUs are frequently scheduled on and utilized with GPU utilization rates of around 51% and 40%, respectively. In contrast, H100 GPUs are still being underutilized with a low mean/median utilization of 20%. Notably, some of them are not being scheduled at all as shown by the utilization data. This is partly because H100 GPUs are still in an early deployment period at the time of this work.

## 3 Methodology

### 3.1 Data Source

Our analysis is performed on data collected from *Delta* over 855 days from January 2022 to May 2024. This section describes data sources for *Stage I*: data collection and extraction in the pipeline in Figure 4.

**System logs.** System logs (202 GB) collected from all compute nodes capture events across system components. We created a set of regular expression (RegEX) patterns and use it to extract GPU error-recovery log entries by referring to NVIDIA XID messages [34] from the system logs (Figure 4-(1)). The GPU error logs are our major sources of error and recovery information.

**Slurm scheduler database.** *Delta* HPC uses the Slurm Workload Manager [61] (Slurm scheduler hereafter) for scheduling user jobs. The Slurm scheduler database keeps track of user job scheduling events, including the start and end times, the scheduled nodes, resource usage, job status, exit codes, and the slurm command line. We use Slurm database for user application failure characterization.

### 3.2 Data Processing Pipeline

This section focuses on *Stage II and III* of the pipeline in Figure 4, which pre-process the raw logs, compute error counts, mean time between errors, error persistence, error propagation, and error impact on user jobs.

### Algorithm 1: Error Coalescing and Persistence Analysis.

**Input** : Error logs with timestamps  $E = \{(e_1, t_1), \dots, (e_n, t_n)\}$ , regex patterns  $\mathcal{R} = \{r_1, r_2, \dots\}$ , time window  $\Delta t$   
**Output**: Coalesced errors with persistence duration  $E'$

```

 $E' \leftarrow \emptyset$  // Initialize output set
foreach pattern  $r \in \mathcal{R}$  do
     $E_r \leftarrow \{(e_i, t_i) \in E \mid e_i \text{ matches } r\}$  // Filter errors with regex
     $i \leftarrow 1$ 
    // Loop through errors in a matched group
    while  $i \leq |E_r|$  do
         $(e_{\text{first}}, t_{\text{start}}, t_{\text{latest}}) \leftarrow (e_i, t_i), t_i$ 
        // Loop through later errors within the matched group
        while  $i + 1 \leq |E_r|$  do
             $(e_{\text{next}}, t_{\text{next}}) \leftarrow (e_{i+1}, t_{i+1})$ 
            // Error has identical message and is close in time
            if  $e_{\text{next}} = e_{\text{first}}$  and  $t_{\text{next}} - t_{\text{latest}} \leq \Delta t$  then
                 $t_{\text{latest}} \leftarrow t_{\text{next}}$  // Discard latest error
                 $i \leftarrow i + 1$ 
            else
                break
        // Store coalesced error and persistence duration
        Add  $(e_{\text{first}}, t_{\text{start}}, t_{\text{latest}} - t_{\text{start}})$  to  $E'$ 
         $i \leftarrow i + 1$  // Move to the next unprocessed error
    return  $E'$ 

```

**Error Coalescing and Persistence Analysis.** The error coalescing step in Figure 4-(1) further filters out duplicated errors. While most errors are logged as isolated events, there are frequent periods where the same error is logged repeatedly in close succession, resulting in error bursts. During these bursts, the system continually detects and attempts to recover from errors, which could lead to system recovery, or failure if unrecoverable. To prevent over-counting, we assume that identical error logs within a short time interval ( $\Delta t$ ) from the same GPU are originated from the same issue. Thus, the error coalescing step counts only the first occurrence by combining identical error log lines from the same GPU within a pre-defined time interval ( $\Delta t$ ) into a single error (see Algorithm 1). The remaining analyses in this paper are conducted on errors after coalescing.

In addition, for each error, we record the time it persists, which we define as an *error persistence duration* (Figure 4-(3)). A longer error persistence duration suggests more time-consuming error recovery or prolonged failure response. We analyzed the error persistence by varying  $\Delta t$  from 5 to 20 seconds and did not observe a notable difference in the result. Hence, we chose  $\Delta t$  to be 5 seconds for subsequent analysis due to computational efficiency. Additionally, since we rarely observe errors lasting more than a single day, we set a maximum persistence cut-off of one day (86,400 seconds) to optimize computational efficiency further.

**Error Statistic Metrics.** Using the coalesced error logs as input, the pipeline computes standard error statistics metrics such as the count and the mean time between errors (MTBE) as in [9] (Figure 4-(2)). In addition, we also compute per-node MTBE by normalizing the error count using the number of GPU nodes in *Delta*. The per-node MTBE indicates the operational hours a single *Delta* GPU node can function before encountering an error.

**Error Propagation Analysis.** We perform error propagation analysis (Figure 4-(4)) to capture how errors propagate within a

GPU and across different GPUs while measuring the propagation time. The propagation probability from GPU error  $e_1$  to  $e_2$  is defined as:

$$P(e_2|e_1) = \frac{\#e_2}{\text{Total } \#e_1}, \quad t_{e_2} - t_{e_1} \leq \Delta t.$$

A propagation path is created if  $e_2$  occurs immediately after  $e_1$  within a predefined time window  $\Delta t$ . If there is no succeeding error  $e_2$  after  $e_1$  within  $\Delta t$ , then  $e_1$  is a terminal error that does not propagate.

For intra-GPU<sup>6</sup> propagation, we require errors  $e_1$  and  $e_2$  to be on the same GPU device, whereas, for the inter-GPU propagation,  $e_1$  and  $e_2$  are from two distinct GPUs on the same node. We additionally record the time difference between the initial ( $e_1$ ) and subsequent errors ( $e_2$ ), referred to as the *propagation time*, for each propagation event. A shorter propagation time suggests a higher correlation between  $e_1$  and  $e_2$ .

**User Job Impact Analysis.** The user job impact analysis step (Figure 4-(5)) associates GPU errors with failed user jobs in order to characterize the impact of GPU errors on user jobs. Section 5 provides the detail of this analysis.

## 4 Characterizing GPU Resilience

This section characterizes the resilience of *Delta*'s NVIDIA A40 and A100 GPUs. Specific resiliency metrics we discuss include error statistics, error persistence distribution, and error propagation of NVIDIA GPU errors in three categories: (a) GPU hardware, (b) NVLink, and (c) GPU memory, as described in Section 2.2 and Table 1. These errors are critical because they propagate to user job, as we show in Section 5. We first highlight key findings from our analysis and then discuss GPU error statistics, error persistence distributions, and error propagation for each of the three error categories.

Separately, we highlight emerging results from the H100 GPUs that are still in the pre-operational phase in *Delta* (see Section 6). Note that we do not directly compare *Delta* with Blue Waters [9], Titan [30], or Summit [36] due to the significant generational gap between GPUs that are used in those machines.

**GPU resiliency in the context of SWOs.** System-wide outages (SWOs) are not the primary focus of this paper; therefore, we provide only a brief description of SWOs in *Delta*. An SWO is a significant downgrade in system operations that slows communication and computation, requiring the SREs to restart the system. This could be due to component failures (e.g., Lustre file system), network congestion, or other causes, such as urgent security updates to GPU drivers requiring a full system reboot. Eight system-wide outages were posted in public status updates over the measurement period of the study. One outage was due to a tornado causing power fluctuation, two outages were due to file system errors, three outages were due to networks, and two others were due to maintenance. Although GPU errors are reported in the SRE's notes, none of the SWOs resulted from a GPU error or failure.

### 4.1 Result Highlights

Our analysis highlights are as follows. Detailed analysis is presented in subsequent sections.

<sup>6</sup>GPU devices are identified by their node ID and PCI Express bus address.

(i) Uncontained memory errors, MMU errors, NVLink errors and GSP RPC timeouts are the predominant errors, accounting for over 99% (62,904 out of 63,253) of the characterized GPU errors (see Table 1); These errors can lead to a GPU error state, causing interruptions to user jobs.

(ii) Contrary to common beliefs, GPU memory is over 30× more reliable regarding MTBE than GPU hardware. Among the GPU hardware components, the newly introduced GSP, intended as a performance enhancer for offloading critical CPU driver tasks, is the most vulnerable due to its lack of robust detection and recovery. Our analysis shows that over 99% of GSP error puts the GPU in an error state, leading to job failure if encountered. In addition, a GSP error requires a GPU reset or a node reboot with significant overheads.

(iii) PMU SPI communication error propagates downstream and causes MMU errors with a probability of 0.82, which then, in turn, results in a job failure almost 100% of the time. Although PMU SPI communication error is a high-impact error from a user job perspective, it is not highlighted in NVIDIA's Developer's Manual [34].

(iv) Despite error detection mechanisms such as CRC and recovery mechanisms such as message retransmitting, NVLink GPU interconnect errors are frequent (2,987 total NVLink errors), with an MTBE of 1415.2 node hours (6.87 system hours); 14% (418) of the NVLink errors affected two or more GPUs. Although the manual indicates that a GPU reset or a node reboot is required, in our measurements, once encountered, an NVLink error has a 66% chance of leading to a job failure. Compared to GSP errors, which render the GPU inoperable for 100% of the time when encountered, NVLink is more resilient to error. Additionally, when an NVLink error is observed but does not affect an application, it may be because NVLink is primarily used for communication rather than computation in many jobs or because multiple NVLink errors within the same job consolidate their impact, resulting in high occurrence rates but minimal application disruption.

(v) Row remapping and error containment mechanisms (see Section 2.3) improve GPU memory resilience and reduce service interruption [32]. Our analysis shows that these mechanisms contain the DBE with a probability of 0.7. However, failure in error containment manifests as uncontained memory errors that can be bursty and persisting in nature, presenting a resilience challenge. In one case, uncontained memory error persisted for 17 days (May 5<sup>th</sup> to May 21<sup>st</sup> 2022) without recovery, generating over a million duplicated log entries that were potentially disruptive.

### 4.2 Error Statistics

Table 1 summarizes the selected GPU error statistics, including error count, mean time between errors (MTBE), and error persistence. During the characterization period, *Delta* recorded 63,253 GPU errors with an MTBE of 67 node hours.

We observed that:

(i) Uncontained memory errors (61%), MMU errors (30%), NVLink errors (5%), and GSP RPC timeout errors (3%) together account for ~99% of GPU-errors that are not induced by user jobs. Uncontained memory errors have the shortest MTBE of 108.7 node hours, followed by MMU errors, NVLink errors, and GSP RPC timeout errors, which have MTBEs of 223.9 hours, 1415.2 hours, and 1979.0 hours,

**Table 1: Delta NVIDIA Ampere GPU resilience statistics.**

| Event Code | Abbr.                        | Category      | Description   | Recovery Action   | Count  | MTBE (hrs) |          | Persistence (s) |       |        |
|------------|------------------------------|---------------|---|---|--------|------------|----------|-----------------|-------|--------|
|            |                              |               |   |   |        | All Nodes  | Per Node | Mean            | P50   | P95    |
| XID 31     | MMU Error                    | Hardware      | GPU memory management unit (MMU) error.   | MMU error due to invalid memory access or driver/hardware bugs.                     | 18,876 | 1.09       | 223.94   | 2.85            | 2.80  | 5.80   |
| XID 48     | DBE                          | Memory        | Double bit ECC memory error (DBE).  | Triggers RRE; GPU reset or node reboot is needed to clear this error if RRE failed. | 32     | 641.25     | 132097.5 | 0.14            | 0.12  | 0.24   |
| XID 63     | RRE                          | Memory        | Row remapping event, triggered by 1 DBE or 2 SBE at the same memory address.  | GPU reset needed for row remapping.   | 95     | 216        | 44496    | 0.12            | 0.12  | 0.12   |
| XID 64     | RRF                          | Memory        | Row remapping failure of a row remapping event.   | A GPU reset is needed to clear this error.  | 35     | 586.29     | 120774.9 | 8.88            | 2.90  | 26.65  |
| XID 74     | NVLink Error                 | Inter-connect | NVLink error, indicating connection issues between GPUs via NVLink interconnection.   | GPU reset or SRE intervention required.   | 2,987  | 6.87       | 1415.2   | 0.76            | 0.24  | 1.18   |
| XID 79     | GPU Fallen Off the Bus Error | Hardware      | GPU has fallen off the system bus and is not reachable, which is typically caused by driver or hardware errors.   | GPU reset or SRE intervention required.   | 31     | 661.94     | 136358.6 | 2.71            | 0.25  | 12.03  |
| XID 94     | Contained Memory Error       | Memory        | Uncorrectable contained ECC error, indicating a successful uncorrectable error containment that prevents error propagation by terminating the affected processes. | Not specified.  | 28     | 732.86     | 150968.6 | 0.12            | 0.12  | 0.14   |
| XID 95     | Uncontained Memory Error     | Memory        | Uncontained memory error, indicating an unsuccessful uncorrectable error containment.   | GPU reset or SRE intervention required.   | 38,905 | 0.53       | 108.69   | 860.24          | 75.22 | 340.69 |
| XID 119    | GSP Error                    | Hardware      | NVIDIA GPU Systems Processor (GSP) error. GSP is a coprocessor that manages GPU initialization and other tasks.   | GPU reset or SRE intervention required.   | 2,136  | 9.61       | 1979.0   | 12.14           | 0.03  | 100.85 |
| XID 122    | PMU SPI Error                | Hardware      | PMU SPI RPC read failure, indicating a failed communication with the PMU.   | Not specified.  | 128    | 160.31     | 33024.4  | 0.05            | 0.06  | 0.08   |

\*An NVIDIA Ampere architecture GPU supports page retirement and up to 512-row remappings (PRE), while previous generations support only 64-page retirements.

\*Row remapping, Contained memory Error, and Uncontained memory Error are new resilience features introduced in the NVIDIA Ampere architecture for uncorrectable memory error management.

\*Event persistence unit: “s” stands for seconds and “p” stands for percentile.

\*All XID events presented, except for Row Remapping Events, are errors. However, for simplicity, we treat all XID events as errors in the scope of this paper.

\*Per node MTBE in hours is derived by multiplying system MTBE with the number of GPU nodes, which is 206 total Ampere GPU nodes.

all in node hours, respectively. Therefore, these are the most critical GPU errors and are studied in depth in this section<sup>7</sup>.

(ii) GPU hardware and interconnect are less resilient than GPU memory, as shown by a lower MTBE of 800 node hours, accounting for GSP, PMU SPI, NVLink, and GPU Fallen Off the Bus errors, compared to GPU memory-related errors: DBEs (double-bit memory errors), RREs (Row Remapping Event), and RRFs (Row Remapping Failures) which has a combined MTBE of 26,093 node hours. In other words, GPU memory is 30× more resilience than the GPU hardware.

(iii) Uncontained memory error, DBE, and RRF are only observed on a few GPUs with the overwhelming majority of these errors occur during the testing phase, thus reaffirming the value of early system stress test to replace defective GPUs. For example, we found

<sup>7</sup>MTBE in terms of system hours can be found in table 1.

that over 90% of the 38,000+ uncontained memory error originated from a few GPUs. Note that we exclude Uncontained memory error in the MTBE comparison between GPU memory and GPU hardware in (ii) above due to this reason.

### 4.3 GPU Error Persistence Distributions

Since the exact GPU recovery timing information is unavailable, error persistence duration, calculated in Algorithm 1, is used as a proxy for the time needed for error recovery or to reach a failure state. A long error persistence duration indicates that an error requires a long recovery time during which the GPU performance or useful computation may be reduced. Table 1 summarizes error persistence duration distributions mean, 50<sup>th</sup> percentile, and 95<sup>th</sup> percentile for each error. By summing up the persistence duration of GPU errors across all GPUs, we calculate the loss of useful GPU

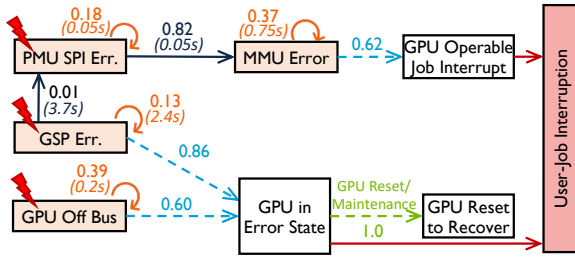


**Figure 5: Intra-GPU hardware errors propagation probabilities. Numbers on the edges show propagation probabilities and average propagation time in seconds (in parentheses).**

computation due to all GPU errors to be 320 GPU hours (13 days), across all GPUs. Although the tail probabilities are quite small, the loss of GPU hours due to errors at the tail (errors persisting longer than p95) is 291 GPU hours, accounting for 91% of the useful GPU computation lost. Note that the 320 hours is an optimistic estimate because it assumes that GPUs could be reset individually and become available to execute user jobs instantly. However, resetting a single GPU in a multi-GPU node requires reloading drivers and additional software. In practice, *Delta*'s SREs reset the entire GPU node to maintain software state consistency. This action has a more significant impact on useful GPU computation for jobs due to higher overheads, e.g., time to allow all executing applications to complete, time spent on node maintenance, and rebooting that can take up to 48 hours for *Delta*. The user job Section 5 further addresses this impact on GPU availability.

Our discussions with *Delta* operational staff confirmed that the long persistent errors usually require manual GPU reset, or if they propagate to other nodes, could result in SWO. However, they emphasized that the SWO due to GPU errors has not yet been observed. The foregoing analysis suggests that SREs should continuously monitor the errors at the tail of the GPU error persistence distribution, i.e., with long persistence duration, to mitigate the error as soon as possible and prevent further loss of GPU hours. A potential solution would be to develop an ML model (e.g., a Bayesian model) to predict the onset of these long persisting errors for preventive actions.

#### 4.4 GPU Error Propagation

This section describes results on both *intra-GPU* and *inter-GPU* error propagation. Understanding GPU error propagation reveals resilience weak links between GPU components. We break down the error-recovery propagation into three categories for the GPU errors listed in Table 1: (a) GPU hardware, (b) NVLink interconnect, and (c) GPU memory. We estimate the propagation probabilities from GPU error logs (see Section 3.2). The three propagation paths in Figures 5 to 7 are highlighted by the lightning signs that indicate the beginning of each path. A close time proximity between two subsequent errors (as depicted on Table 1) suggests causality.

**4.4.1 GPU Hardware.** Figure 5 shows error propagation across GPU hardware components. We found three dominant GPU hardware error propagation paths, originating with (i) the GSP (GPU

System Processor) RPC Timeout Errors, (ii) PMU (Power Management Unit) SPI Communication Errors, and (iii) GPU Fallen Off the Bus Errors.

**GSP RPC Timeout Errors.** Error propagations originating with GSP RPC timeout errors are the most prominent among GPU hardware errors (see table Table 1). A GSP RPC timeout error arises when the GSP fails to respond to the remote procedure calls from the GPU driver. Figure 5 shows that, with a probability of 0.99, GSP errors lead to the recurrence of the same error or put the GPU in an inoperable state. The remaining 0.01 (21 cases in our data set) of GSP RPC timeout errors caused PMU SPI communication errors (see the follow-up description) that led to user job failure, as depicted in Figure 1. More in-depth analysis of our data shows that 99% of GSP PRC Timeout errors appeared in isolation without a preceding error.

GSP RPC timeout errors can be caused by either GSP firmware bugs [33] or a highly demanding workload. For example, *Delta* SREs observed that these errors were highly correlated with demanding GPU ML benchmarks. *Delta* SREs indicate that GSP RPC timeout errors are high-impact errors that require manual node reboots to recover. Our analysis confirms that the GSP is a single point of failure on the Ampere GPUs in part due to their spontaneous nature and high downstream impact (e.g., GPU hangs) on the GPU.

**PMU SPI Communication Errors.** Communication errors with the power management unit (PMU) over the Serial Peripheral Interface (SPI), known as *PMU SPI errors*, can cause power management issues (e.g., inability to change the core frequency). In our data we observe that this type of errors can lead to MMU errors with a probability of 0.82 (see Figure 5), ultimately leading to user job failures. The rest (0.18) of the PMU SPI errors resulted in another PMU SPI error in close succession, leading to persisting error patterns. We observed 128 occurrences of PMU SPI errors (see Table 1) with a 0.97 probability of leading to user job failures (see Table 2).

**GPU Fallen Off the Bus.** GPU Fallen Off the Bus errors were logged when the GPU driver could not reach the GPU over the PCI-E/SMX system bus interface. This error is an integration error often due to loose GPU-motherboard connection or contact failure because of thermal cycles [52].

Our *GPU hardware error propagation* analysis suggests that the error detection and recovery of GSP, PMU, and the communication interfaces (e.g., PMU SPI) need to be improved via duplication and error-detection and correction mechanism to prevent single-points of failure. In fact, AWS recommends disabling GSP for stability over performance benefits [35]. A more well-rounded solution, such as improving GSP SW and HW reliability while maintaining performance benefits, needs to be investigated. Moreover, additional detection and recovery mechanisms are needed to detect integration-related errors such as GPU Fallen Off the Bus errors.

**4.4.2 NVLink Interconnect.** NVLink is an intra-node GPU-to-GPU interconnect for communications and data exchanges. An NVLink error can impact a single or multiple GPUs on the same node, possibly rendering the entire multi-GPU compute pool unavailable (see Figure 6). We observed both kinds of propagation from our error logs.

**NVLink Inter-GPU Propagation.** An NVLink error occurs when one or more NVLinks experience an error. Our analysis shows

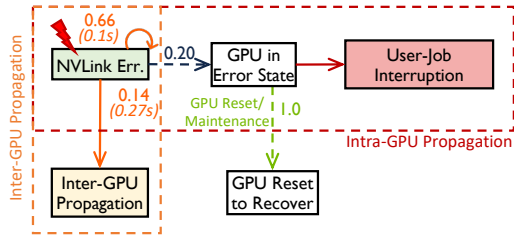


Figure 6: NVLink intra-GPU and inter-GPU error propagation. Numbers on the edges show propagation probabilities and average propagation time in seconds (in parentheses).

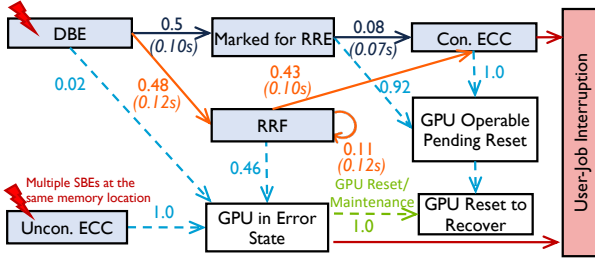


Figure 7: Intra-GPU uncorrectable memory error recovery paths. Numbers on the edges show propagation probability with average propagation time in seconds (in parentheses).

that 84% of the ~3,000 NVLink errors did not propagate across GPUs, and the other 16% involved two or more GPUs of the same compute node; 5% of NVLink errors involved 4 or more GPUs, and 35 NVLink errors affected all eight GPUs on the 8-way A100 GPU nodes. GPU resets are needed to recover from NVLink errors, and, as with GPU hardware errors, we found no preceding hardware errors before NVLink errors, making them less detectable or predictable than memory-related errors. The results indicate that while the percentage of NVLink errors that propagate is small, the numbers are significant, especially in 8-way GPU nodes.

**NVLink Intra-GPU Propagation.** NVLink errors, similar to GPU hardware errors, happen in isolation without preceding errors. An NVLink error either leads to another NVLink error within close succession (probability of 0.66), propagates to neighboring GPUs (probability of 0.14) or leaves the faulty GPU in an error state (probability of 0.20) that requires a GPU reset.

In addition, we observed 23 cases of NVLink errors that led to job failures. Figure 8-Example 1 shows one such case, in which an NVLink error on one GPU led to an MPI error, and ultimately the failure of a user job that was scheduled on four GPUs across four different nodes.

**4.4.3 GPU Memory.** Intra-GPU uncorrectable memory error recovery paths are shown in Figure 7. SBEs are omitted because ECC automatically corrects them and are not logged.

**DBE Error Recovery Path.** As shown in Figure 7, row remapping recovery (RRE) triggered by a DBE has a success rate of 0.5. For the remaining row remapping events that fail (RRF), the GPU still contains the DBE by terminating only the affected user jobs and

| Incident 1: NVLink Error Caused App Failure  | Incident 2: PMU SPI Error Caused App Failure   |
|--|--|
| <pre>[scheduler][slurmctlid][2023-07-26T19:18:28] Job started in 'gpuA100x4' partition on gpus[012,034,066,095]. [JobId=2220507]</pre> | <pre>[scheduler][slurmctlid][2022-11-21T10:57:50] Job started in 'gpuA100x4' partition on gpus[022]. [JobId=1174830]</pre>         |
| <pre>[gpua034][kernel][2023-07-26T19:18:37] Critical NVLink error detected. [ErrorCode=XID 74, Link=10, PCI=0000:07:00]</pre>          | <pre>[gpua022][kernel][2022-11-21T11:01:20] SPI read failure at address 141952. [ErrorCode=XID 122]</pre>                          |
| <pre>[gpua034][slurmstepd][2023-07-26T19:18:41] MPI error handler invoked (due to NVLink failure). [JobId=2220507, Status=-25]</pre>   | <pre>[gpua022][kernel][2022-11-21T11:01:20] MMU Fault detected on ENGINE GRAPHICS. [ErrorCode=XID 31, AccessType=VIRT_WRITE]</pre> |
| <pre>[scheduler][slurmctlid][2023-07-26T19:18:41] Job completed with segmentation fault. [JobId=2220507, ExitStatus=139]</pre>         | <pre>[scheduler][slurmctlid][2022-11-21T11:01:21] Job completed with error. [JobId=1174830, ExitStatus=1]</pre>                    |

Figure 8: Incidents of GPU errors leading to job failure.

offlining the faulty page. The error containment process succeeded for 43% of the time after an RRF, and the GPU remains operable until the next maintenance window. Otherwise, if error containment is not triggered after an RRF (46% of the time), the GPU enters an inoperable error state, requiring a reset. Overall, considering both DBE recovery paths (RRE and error containment after an RRF), the impact of DBEs is alleviated 70.6% of the time, with GPU remained operable. This is not achievable on previous generation GPUs (e.g., Kepler in [9, 52]) as a DBE immediately causes user job interruption and GPU failure, requiring GPU reset to recover [34]. Only one case was found where a DBE lacked a succeeding RRE or RRF, possibly due to logging issues. Most DBEs and RRFs occurred during *Delta*'s testing phase, affecting six (0.71%) and four (0.47%) of 848 Ampere GPUs, respectively. These GPUs were likely replaced by SREs afterward.

**Unsuccessful Error Containment.** The memory error containment can fail, resulting in uncontained memory errors (Section 2.3). Those errors do not have preceding or succeeding errors (see Figure 7), suggesting that multiple SBEs caused the uncontained memory errors in our data. Moreover, uncontained memory errors are highly bursty and persistent and may spam the console logs, consuming useful compute cycles and leaving the GPU inoperable. We found an example where an error occurred for 17 consecutive days (May 2022) before it was resolved. Uncontained memory errors must be cleared by manual GPU resets [32]. Finally, only 4 GPUs (0.47%) in *Delta* experienced uncontained memory errors, and one GPU contributed to 99% of all those errors.

Our analysis suggests that new memory error recovery mechanisms on Ampere GPUs are effective and the impact of DBEs are alleviated for 71% of times. However, the highly bursty and persisting nature of uncontained memory errors can lead to node/system operation disruptions, presenting a challenge.

## 4.5 Examples of Error Propagation to User Jobs

Figure 8 presents two more incidents in which GPU errors led to user job failures, in addition to the one described in Figure 1. Section 5 presents a more systematic user job failure characterization and correlations with GPU errors.



**Incident 1:** An NVLink error on a single node disrupted a user job scheduled across four nodes. During execution, one of the GPUs on the node being scheduled encountered an NVLink error, which resulted in an MPI NVLink error, and the GPU required a manual GPU reset to recover. As the user job required all four GPUs (on four different nodes in this case) to run, one malfunctioning GPU caused the entire job to fail with a segmentation fault (EXITSTATUS 139). This incident shows that an NVLink error can potentially impact all user jobs associated with the faulty node.

**Incident 2:** In this incident, the GPU running the user job experienced a PMU SPI error, subsequently leading to an MMU error. As stated in Section 4.4, the exact reason that causes this is unknown. Based on existing literature and developer blogs, a PMU SPI error can lead to an MMU errors because an error in communication with the PMU causes failures in MMU power management/frequency scaling. This incident shows that peripheral hardware such as PMU and its communication channel (SPI) are critical resilience weak links that can cause GPU and user job failure.

## 5 Propagation of Faults to Jobs

This section provides an in-depth analysis of job-level fault tolerance and resulting GPU downtime. A GPU error can lead to:

- (1) *Job Failure:* A GPU error may not be handled by jobs, either because the error itself is not contained or because of lack of appropriate error handling mechanisms. For example, GSP errors lead to a GPU failure and requires a node reboot. To recover from such failures, jobs need to be re-executed from the beginning or rolled back to the closest checkpoint, and
- (2) *GPU Downtime:* Downtime can occur when GPUs need to be reset or replaced by the operator, and no jobs can be scheduled on the GPU in the interim.

### 5.1 Result Highlights

Figure 9 and Table 2 show the overall impact of hardware errors on applications. In summary, we observe that:

(i) Except for MMU and NVLink errors, no other hardware errors are handled by jobs, thus resulting in their failure. Therefore, there is a need to improve the reliability of underlying hardware to minimize such failures. While checkpointing is an option, checkpointing routines have high overhead up to 40% [29, 56, 57] including management, storage, and restore.

(ii) The overall availability per GPU node is ~99.5%, corresponding to a downtime of 7 minutes per day. This level of unavailability suggests that even if the rest of the infrastructure is highly available, current GPUs may not provide sufficient level of availability needed to meet the demands of critical applications. Additionally, we project the impact of this availability distribution at increased scales (for both node scale and job duration) with emulation and find that significant over-provisioning between 5–20% would be necessary to handle associated failures. Improving GPU availability to 99.9% can lead to a reduction in over-provisioning from 20% to just 5% (as explained in further detail in Section 5.4).

### 5.2 Job Statistics

During the characterization period, there were 1,445,119 user jobs submitted to GPU nodes, with a success rate of 74.68%, and 1,686,696

jobs submitted to CPU nodes, with a similar success rate of 74.90%. About 69.86% of user jobs ran on a single GPU, 27.31% on 2-4 GPUs and only 2.83% of jobs used 4 GPUs or more.

Due to lack of specific information on whether a job is ML-related, we estimate the percentage of ML user jobs based on a job submission name and system modules/libraries imported.<sup>8</sup> For instance, user jobs with names containing `model` or `train` are likely related to machine learning. We provide detailed statistics on node hours used and durations for both job types in Table 3.

## 5.3 Job Failure Analysis

To understand job failure patterns, we first separate jobs into “Completed” and “GPU-Failed” depending on their completion status. Based on this job categorization, we analyze: (i) GPU errors that most likely lead to a job failure, and (ii) the potential recovery strategies such as check-pointing and exception handling.

*Classifying Job Runs:* We classify jobs based on their exit status and proximity of job failure time to GPU error occurrence time. The job exit status is obtained from the Slurm job scheduler logs (as described in Section 3.1). We mark a job as “GPU-failed” if a GPU error occurs within a twenty-second interval before job failure.

*Correlating GPU Errors and Job Failures:* We breakdown all GPU-failed jobs by specific GPU errors that most likely lead to the job failure. Table 2 provides probabilities of user jobs failures per GPU errors. As any of the encountered errors may have contributed to the job failure, we consider all GPU errors occurring within the 20-second interval to be responsible for the failure.

Overall, other than NVLink and MMU errors, all GPU errors such as ECC errors, GSP RPC timeout, and PMU failures propagate (as discussed in Section 4.4) and cause a job failure. NVLink and MMU errors do not necessarily lead to a job failure because:

- (1) for *NVLink errors*, the link or GPU may not be in use by any user jobs (as discussed in Section 4.4)<sup>9</sup>, and
- (2) for *MMU errors*, there can be application or library-level masking mechanisms. Besides hardware errors, MMU errors can also

<sup>8</sup>We do not use the exact submission script to classify job types due to privacy restrictions.

<sup>9</sup>Based on our understanding, NVLink errors can occur even when no workload is running [13].

| XID | GPU Error            | # GPU-failed jobs encountering given XID | #Jobs encountering given XID | Job Failure Probability given an XID Error (%) |
|-----|----------------------|--|------------------------------|--|
| 31  | MMU Err.             | 3760                                     | 6408                         | 58.67  |
| 95  | Uncon. ECC           | 514                                      | 529                          | 97.16  |
| 122 | SPI PMU RPC failure  | 57                                       | 59                           | 96.61  |
| 119 | GSP RPC Timeout      | 36                                       | 36                           | 100.00   |
| 74  | NVL Err              | 23                                       | 35                           | 65.71  |
| 48  | GPU DBE              | 9  | 10                           | 90.00  |
| 64  | Row remapping failed | 8  | 8                            | 100.00   |
| 94  | Contained ECC        | 3  | 3                            | 100.00   |
| 63  | ECC Page Retirement  | 1  | 2                            | 50.00  |

**Table 2: Distribution of GPU-failed jobs across the different GPU error types. The failure probability is calculated as (# GPU-failed jobs encountering that GPU error) / (# Jobs encountering that GPU error). The total number of GPU-failed jobs is 4,322 during the 2.5-year characterization period.**

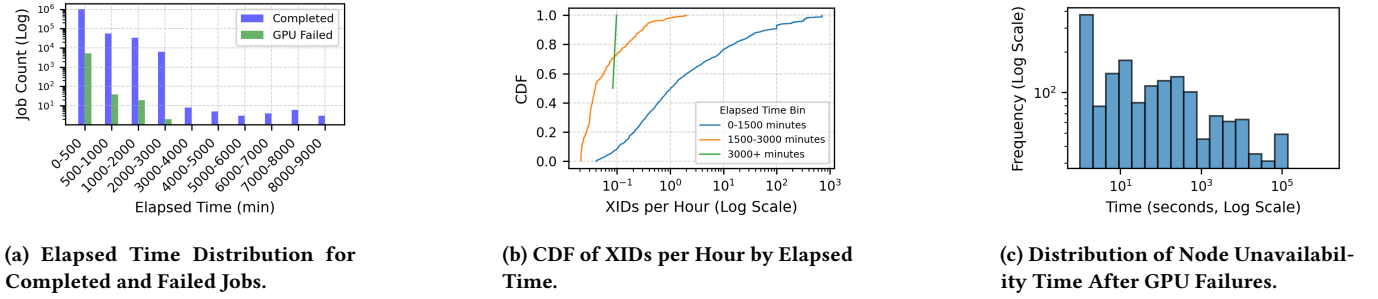


**Figure 9: Summary of GPU-related Metrics: Elapsed Time Distribution, XID CDF, and Unavailability Time Distribution.**

occur when a buggy user code makes illegal memory accesses that cannot be mapped in the virtual-to-physical address space. These errors can be managed using appropriate application-level exception handlers. Popular libraries and frameworks for machine learning [40–42] have support to handle such exceptions by skipping the associated training iteration, albeit at the cost of model quality.

*Job Recovery Strategies:* We further analyze the impact of job duration on failures. While there are other failures due to user bugs, network, and filesystem errors, we do not consider them as this paper primarily focuses on GPU errors. Figure 9a shows the number of completed and GPU-failed jobs versus the system time spent executing a job. We find that job failures are prevalent for shorter-duration jobs (less than 4000 minutes) and lead to a total loss of 7,500 node hours.

Figure 9b shows the distribution of number of GPU errors encountered versus job duration for both successful and failed jobs. While jobs that execute for more than 4,000 minutes (~3 days) face multiple GPU errors, they do execute to completion. A more in-depth analysis revealed that majority of these GPU errors are MMU errors that typically occur with incorrect memory accesses and often disappear under retries. Typically long running jobs tend to have mechanisms such as checkpointing to recover from these memory errors.

In summary, while most hardware errors lead to job failures, a few jobs have associated exception handling mechanisms that provide fault tolerance by either restoring checkpoints or by gracefully exiting. However, for jobs such as ML that recover by skipping training iterations, output quality could be impacted.

### 5.4 Impact of GPU Downtime on Jobs

While significant node hours might be lost due to wasted compute time, additional node hours are also lost due to the time required to recover the impacted GPU node, either by resetting the GPU node or replacing it entirely. To reset the GPU node, operators typically drain the node i.e. wait for other jobs running on the node to complete and then reboot. After the reboot, if the node successfully passes the health check, the node reset is successful and new jobs can be scheduled on the GPU node. If the reset is unsuccessful, the node is marked failed until the GPU is physically replaced. To calculate the average system downtime, we estimate the total time when the GPU is unavailable which primarily includes the drain

| GPU Count | Count (%)         | Elapsed Time (minutes) |       |         | GPU Hours (k) |        |
|-----------|-------------------|------------------------|-------|---------|---------------|--------|
|           |                   | Mean                   | P50   | P99     | ML            | Non-ML |
| 1         | 1,013,170 (69.86) | 175.62                 | 10.15 | 2483.12 | 241.6         | 2724.0 |
| 2-4       | 396,133 (27.31)   | 145.04                 | 4.75  | 2880.03 | 344.6         | 3108.7 |
| 4-8       | 22,474 (1.55)     | 133.89                 | 2.70  | 2880.20 | 57.9          | 338.6  |
| 8-32      | 15,440 (1.07)     | 270.40                 | 73.73 | 2880.17 | 107.1         | 1332.7 |
| 32-64     | 2,054 (0.14)      | 204.52                 | 10.25 | 2817.08 | 161.9         | 226.4  |
| 64-128    | 913 (0.063)       | 226.28                 | 0.32  | 2211.94 | 25.1          | 322.3  |
| 128-256   | 82 (0.006)        | 226.53                 | 9.19  | 2785.29 | 0.0           | 52.4   |
| 256+      | 25 (0.002)        | 32.12                  | 20.40 | 120.14  | 0.0           | 4.5    |

**Table 3: Job distribution, elapsed time statistics (Mean, P50, P99), and GPU hours divided into ML and Non-ML categories for various GPU configurations.**

and reboot time. Figure 9c shows the distribution of the unavailable time across the entire characterization duration. Overall, we find that the expected time to service the failed node is 0.3 hours and a total of 5,700 node hours are lost due to GPU downtime. Using the node downtime and failure distributions, we can estimate the availability of the GPU node as  $\frac{MTTF}{MTTF+MTTR} = 99.5\%$ , where node MTTF is 67 hours<sup>10</sup> and MTTR is 0.3 hours.

*Project impact of availability on long running and large scale jobs:* While we provide error and recovery statistics in previous sections, we also attempt to determine how these distributions would project to jobs that run on a different system. To do so, we built a simulation tool driven by our analysis. The parameters of the simulation tool can be varied based on the scenario under consideration.

Specifically, we simulate the case where jobs (such as ML training) use the entire system capacity of 800 nodes and run for a duration of 1 month. These jobs require all GPUs to be operational to make progress, and frequent node failures can lead to resource unavailability and slower job progress. When such failures occur, additional provisioning of GPU resources is necessary to allow the job to resume on alternate nodes while the failed nodes recover.

The simulation uses a discrete time event simulation with node failure probabilities derived from our prior analysis. The recovery time after a failure is dependent on variables such as checkpoint load time, availability of spare GPUs, etc. To account for variability introduced by these factors, we parameterize recovery time and

<sup>10</sup>The node MTTF number is estimated from the GPU’s MTBE, in which we conservatively assumes that all GPU errors lead to node interruption.

perform a parameter sweep. For a training job with 800 GPUs, a recovery time of 40 mins and a 1% chance of a single GPU failure per hour, the required over-provisioning is 20%—i.e., 160 additional GPUs are needed beyond the original 800. However, if the recovery time is reduced to 5 mins, downtime decreases significantly, and the required over-provisioning drops to 5%.

This highlights the criticality of minimizing recovery time to reduce downtime for large and long running jobs.

In summary, every GPU node in the system has two nines of availability. While such availability does not significantly impact small jobs that use recovery mechanisms, large jobs can face significant downtime. Significant over-provisioning up to 20% is required to eliminate such downtime.

## 5.5 Lessons Learned: Potential Resilience Improvements

**GPU Resilience.** We perform a counterfactual analysis of potential improvement in GPU resilience by improving the GPU hardware resilience and removing top-offending GPUs as outliers. We see a 3× improvement in MTBE from 67 node hours to 190 node hours if we exclude the top offending GPUs for each GPU error in our calculation. We see an additional 16% improvement in GPU node MTBE to 223 hours by excluding GSP, PMU SPI, and NVLink errors. This counterfactual analysis shows that (i) ruling out defective GPUs by comprehensive testing and continuous GPU error monitoring can substantially improve resilience system-wide, and (ii) improving resilience for peripheral hardware, such as GSP, PMU, and critical communication channels connecting GPU peripheral hardware can improve GPU device MTBE, by up to 16% in our case.

**Benefits to Node Availability and User Jobs.** Assuming that top-offending GPUs and the selected hardware errors are absent, we recompute the node availability and the benefits to user jobs using the updated MTBE of 223 hours. Under this assumption, the availability of the GPU node is improved to  $\frac{MTTF}{MTTF+MTTR} = 99.9\%$  from 99.5%, given that the MTTR is unchanged. For the same training job setting as described in Section 5.4, the projected node availability of 99.9% reduces the overprovisioning from 20% to 5%, a 4× reduction.

## 6 Emerging Errors in H100 GPUs

This section presents early findings on H100 GPU errors in *Delta AI* extension since August 2024, complementing the aforementioned analyses.

**MTBE:** H100 GPUs experienced 18 MMU errors, 10 double-bit errors, 5 row-remapping failures, 9 contained uncorrectable memory errors, and 70 XID 136 events, resulting in a mean time between errors (MTBE) of 4,114 hours. This is likely due to lower utilization, significantly higher than A100 and A40.

**DBE and RRF:** We observed five row-remapping failures (RRFs) and ten double-bit errors (DBEs), which is unusual, as it typically indicates exhausted remappable rows. This observation contrasts with our expected row remapping events (RRE), which signifies successfully resolving/acting upon uncorrectable errors. DBE and RRF indicate potential H100 GPU memory issues, but further monitoring is required.

**XID 136:** This event, the most frequently observed XID error in H100 GPUs, lacks a detailed description in the NVIDIA Manual [34]. Its cause and impact remain to be seen.

## 7 Related Work

Existing work has analyzed GPU resilience at the microarchitecture-, system-, and application-level. This paper extends previous work by comprehensive analyses of GPU error characteristics, failure propagation, and their impact on user jobs.

*Microarchitecture-level GPU Resilience.* Previous research [18, 45, 55, 60] has primarily focused on the resilience of individual GPUs at the microarchitecture and software level, e.g., for older generations such as NVIDIA G80 [5]. However, these works do not evaluate the resiliency of modern GPUs in large-scale HPC settings.

*System-level GPU Resilience in HPC Settings.* Existing studies have analyzed the resilience of GPUs in HPC systems [6, 8, 14, 17, 24], for example, the NVIDIA Tesla K20X GPUs in various supercomputers [9, 15, 16, 30, 31, 37, 52, 53]. The studies on Blue Waters, Titan, and Summit supercomputers [9, 30, 31, 36] have examined node failures and GPU error characteristics. However, these works study previous generations of GPUs with a focus on GPU memory errors. Our work complements those works by providing resilience insights into the latest generation of GPUs, focusing on a broader range of components.

*Application-level GPU Resilience in Data-centers and Deep Learning Workloads.* Recent research has focused on understanding GPU power usage [31], GPU component-level failures [23], software-level error handling [12, 28], and the impact of GPU software errors propagation on GPGPU applications [2, 26, 43, 58] and emerging GPU workloads such as Convolutional Neural Networks (CNNs) [7, 10], Large Language Models (LLMs) [11, 22] and safety-critical applications [38, 47].

*Orthogonal Work Related to GPUs.* Other prior works on GPUs focus on workload analysis [20, 27, 59], scalability [22], memory efficiency [46] and performance [19] without an in-depth discussion of reliability, which is orthogonal to our work.

## 8 Discussion

**Justification of Analyzing Errors:** Data-driven HPC resilience characterization studies analyze operational data on system/application errors to provide insights into system reliability. [8, 9, 15, 16, 30, 31, 36, 37, 52, 53]. While in those studies, the error rate is used as the key metric to quantify reliability, some [3, 50] argue that fault rate is a more appropriate metric.

Errors represent the manifestation of faults and have direct downstream consequences, such as triggering recovery mechanisms, causing application interruptions, or leading to system-wide outages (SWOs). While a fault may result in multiple errors, it is the resulting errors that the recovery mechanisms must address to maintain system health. These errors and their recovery process directly impact system health, performance, and availability. For example, an uncorrectable memory error in A100 GPU memory necessitates row remapping and a GPU reset, reducing node availability. Thus, in the longer term, knowing the underlying fault is valuable for building better systems. However at runtime, the system needs to handle the errors regardless of whether the underlying

fault is permanent or transient [44]. As such, SREs prioritize errors over faults, as errors offer actionable insights into system reliability and can be used to drive recovery actions. Hence, like many others who study operational data, we chose to study errors.

**Potential errors in NVIDIA driver logging:** A potential source of error is the logging inconsistency of the NVIDIA driver between different XID errors. NVIDIA driver is a proprietary software, and its source code is publicly unavailable, making the exact specifications of its error logging mechanism unverifiable. We attempt to minimize the impact of inconsistency to the best of our ability through consistent log data collection and error coalescing. We ensure critical error logs, such as NVIDIA XID errors, are captured from each GPU per compute node, and coalesce multiple errors from the same source within a 5-second window into a single occurrence if they share the same error message (see Section 3.2), reducing both over- and under-counting due to logging inconsistencies.

## 9 Conclusion

This paper described the results of a resilience study of *Delta* consisting of 1,168 NVIDIA GPUs: A40, A100, and H100 GPUs. The study uses two and a half years of data on GPU errors collected across those GPUs. We assessed the resilience of GPU hardware components to evaluate the resilience of various GPU components to failures and their impact on GPU and node availability. We measured the key propagation paths in GPU hardware, GPU interconnect (NVLink), and GPU memory. Finally, we evaluated the impact of the observed GPU errors on user jobs. Future work extends this analysis to the Grace-Hopper GPU-based system, executing jointly complex HPC and ML workloads.

## References

- [1] Md Mahbub Alam, Luis Torgo, and Albert Bifet. 2022. A survey on spatio-temporal data analytics systems. *Comput. Surveys* 54, 10s (2022), 1–38.
- [2] Abdul Rehman Anwer, Guanpeng Li, Karthik Pattabiraman, Michael Sullivan, Timothy Tsai, and Siva Kumar Sastry Hari. 2020. Gpu-trident: efficient modeling of error propagation in gpu programs. In *SC20: International Conference for High Performance Computing, Networking, Storage and Analysis*. IEEE, 1–15.
- [3] Majed Valad Beigi, Yi Cao, Sudhanva Gurumurthi, Charles Recchia, Andrew Walton, and Vilas Sridharan. 2023. A Systematic Study of DDR4 DRAM Faults in the Field. In *2023 IEEE International Symposium on High-Performance Computer Architecture (HPCA)*, 991–1002. <https://doi.org/10.1109/HPCA56546.2023.10071066>
- [4] Peter Braam. 2019. The Lustre storage architecture. *arXiv preprint arXiv:1903.01955* (2019).
- [5] Giani Braga, Marcio M Gonçalves, and José Rodrigo Azambuja. 2023. Software-controlled pipeline parity in gpu architectures for error detection. *Microelectronics Reliability* 148 (2023), 115155.
- [6] Nevin Cini and Gulay Yalcin. 2020. A Methodology for Comparing the Reliability of GPU-Based and CPU-Based HPCs. *ACM Comput. Surv.* 53, 1, Article 22 (Feb. 2020), 33 pages. <https://doi.org/10.1145/3372790>
- [7] Josie E Rodriguez Condia, Juan-David Guerrero-Balaguera, Fernando F Dos Santos, Matteo Sonza Reorda, and Paolo Rech. 2022. A multi-level approach to evaluate the impact of GPU permanent faults on CNN’s reliability. In *2022 IEEE International Test Conference (ITC)*. IEEE, 278–287.
- [8] Nathan DeBardeleben, Sean Blanchard, Laura Monroe, Phil Romero, Daryl Grunau, Craig Idler, and Cornell Wright. 2014. GPU behavior on a large HPC cluster. In *Euro-Par 2013: Parallel Processing Workshops: BigDataCloud, DIHC, FedCI, HeteroPar, HiBB, LSDVE, MHPC, OMHI, PADABS, PROPER, Resilience, ROME, and UCHPC 2013, Aachen, Germany, August 26-27, 2013. Revised Selected Papers 19*. Springer, 680–689.
- [9] Catello Di Martino, Zbigniew Kalbarczyk, Ravishankar K. Iyer, Fabio Baccanico, Joseph Fullop, and William Kramer. 2014. Lessons Learned from the Analysis of System Failures at Petascale: The Case of Blue Waters. In *2014 44th Annual IEEE/IFIP International Conference on Dependable Systems and Networks*. 610–621. <https://doi.org/10.1109/DSN.2014.62>
- [10] Fernando Fernandes dos Santos, Pedro Foletto Pimenta, Caio Lunardi, Lucas Draghetti, Luigi Carro, David Kaeli, and Paolo Rech. 2018. Analyzing and increasing the reliability of convolutional neural networks on GPUs. *IEEE Transactions on Reliability* 68, 2 (2018), 663–677.
- [11] Abhimanyu Dubey, Abhinav Jauhri, Abhinav Pandey, Abhishek Kadian, Ahmad Al-Dahle, Aiesha Letman, Akhil Mathur, Alan Schelten, Amy Yang, Angela Fan, et al. 2024. The llama 3 herd of models. *arXiv preprint arXiv:2407.21783* (2024).
- [12] Bo Fang, Karthik Pattabiraman, Matei Ripeanu, and Sudhanva Gurumurthi. 2014. GPU-Qin: A methodology for evaluating the error resilience of GPGPU applications. In *2014 IEEE International Symposium on Performance Analysis of Systems and Software (ISPASS)*. IEEE, 221–230.
- [13] NVIDIA Forums. 2024. NVLink error 74 fatal error detected. <https://forums.developer.nvidia.com/t/nvlink-error-74-fatal-error-detected/55582/1> Accessed: 2025-02-24.
- [14] Haryadi S Gunawi, Riza O Suminto, Russell Sears, Casey Gollhofer, Swaminathan Sundararaman, Xing Lin, Tim Emami, Weiguang Sheng, Nematollah Bidokhti, Caitie McCaffrey, et al. 2018. Fail-slow at scale: Evidence of hardware performance faults in large production systems. *ACM Transactions on Storage (TOS)* 14, 3 (2018), 1–26.
- [15] Saurabh Gupta, Tirthak Patel, Christian Engelmann, and Devesh Tiwari. 2017. Failures in large scale systems: long-term measurement, analysis, and implications. In *Proceedings of the International Conference for High Performance Computing, Networking, Storage and Analysis*. 1–12.
- [16] Saurabh Gupta, Devesh Tiwari, Christopher Jantzi, James Rogers, and Don Maxwell. 2015. Understanding and exploiting spatial properties of system failures on extreme-scale hpc systems. In *2015 45th Annual IEEE/IFIP International Conference on Dependable Systems and Networks*. IEEE, 37–44.
- [17] Imran S Haque and Vijay S Pande. 2010. Hard data on soft errors: A large-scale assessment of real-world error rates in gpgpu. In *2010 10th IEEE/ACM International Conference on Cluster, Cloud and Grid Computing*. IEEE, 691–696.
- [18] Siva Kumar Sastry Hari, Timothy Tsai, Mark Stephenson, Stephen W Keckler, and Joel Emer. 2015. SASSIFI: Evaluating resilience of GPU applications. In *Proceedings of the Workshop on Silicon Errors in Logic-System Effects (SELSE)*.
- [19] Qinghao Hu, Peng Sun, Shengen Yan, Yonggang Wen, and Tianwei Zhang. 2021. Characterization and prediction of deep learning workloads in large-scale GPU datacenters. In *Proceedings of the International Conference for High Performance Computing, Networking, Storage and Analysis (St. Louis, Missouri) (SC ’21)*. Association for Computing Machinery, New York, NY, USA, Article 104, 15 pages. <https://doi.org/10.1145/3458817.3476223>
- [20] Qinghao Hu, Zhisheng Ye, Zerui Wang, Guoteng Wang, Meng Zhang, Qiaoling Chen, Peng Sun, Dahua Lin, Xiaolin Wang, Yingwei Luo, et al. 2024. Characterization of large language model development in the datacenter. In *21st USENIX Symposium on Networked Systems Design and Implementation (NSDI 24)*. 709–729.
- [21] Chip Huyen. 2022. *Designing machine learning systems*. " O’Reilly Media, Inc".
- [22] Ziheng Jiang, Haibin Lin, Yinmin Zhong, Qi Huang, Yangrui Chen, Zhi Zhang, Yanghua Peng, Xiang Li, Cong Xie, Shihao Nong, et al. 2024. {MegaScale}: Scaling large language model training to more than 10,000 {GPUs}. In *21st USENIX Symposium on Networked Systems Design and Implementation (NSDI 24)*. 745–760.
- [23] Jeageun Jung and Mattan Erez. 2023. Predicting Future-System Reliability with a Component-Level DRAM Fault Model. In *Proceedings of the 56th Annual IEEE/ACM International Symposium on Microarchitecture*. 944–956.
- [24] Apostolos Kokolis, Michael Kuchnik, John Hoffman, Adithya Kumar, Parth Malani, Faye Ma, Zachary DeVito, Shubho Sengupta, Kalyan Saladi, and Carole-Jean Wu. 2024. Revisiting Reliability in Large-Scale Machine Learning Research Clusters. *arXiv preprint arXiv:2410.21680* (2024).
- [25] Baolin Li, Yankai Jiang, Vijay Gadepally, and Devesh Tiwari. 2024. Llm inference serving: Survey of recent advances and opportunities. *arXiv preprint arXiv:2407.12391* (2024).
- [26] Guanpeng Li, Karthik Pattabiraman, Chen-Yang Cher, and Pradip Bose. 2016. Understanding Error Propagation in GPGPU Applications. In *SC ’16: Proceedings of the International Conference for High Performance Computing, Networking, Storage and Analysis*. 240–251. <https://doi.org/10.1109/SC.2016.20>
- [27] Heting Liu, Zhichao Li, Cheng Tan, Rongqiu Yang, Guohong Cao, Zherui Liu, and Chuanxiong Guo. 2023. Predicting GPU Failures With High Precision Under Deep Learning Workloads. In *Proceedings of the 16th ACM International Conference on Systems and Storage*. 124–135.
- [28] Naoya Maruyama, Akira Nukada, and Satoshi Matsuoka. 2010. A high-performance fault-tolerant software framework for memory on commodity gpus. In *2010 IEEE International Symposium on Parallel & Distributed Processing (IPDPS)*. IEEE, 1–12.
- [29] Avinash Maurya, Robert Underwood, M Mustafa Rafique, Franck Cappello, and Bogdan Nicolae. 2024. Datastates-llm: Lazy asynchronous checkpointing for large language models. In *Proceedings of the 33rd International Symposium on High-Performance Parallel and Distributed Computing*. 227–239.
- [30] Bin Nie, Devesh Tiwari, Saurabh Gupta, Evgenia Smirni, and James H Rogers. 2016. A large-scale study of soft-errors on GPUs in the field. In *2016 IEEE International Symposium on High Performance Computer Architecture (HPCA)*.

- IEEE, 519–530.
- [31] Bin Nie, Ji Xue, Saurabh Gupta, Christian Engelmann, Evgenia Smirni, and Devesh Tiwari. 2017. Characterizing temperature, power, and soft-error behaviors in data center systems: Insights, challenges, and opportunities. In *2017 IEEE 25th International Symposium on Modeling, Analysis, and Simulation of Computer and Telecommunication Systems (MASCOTS)*. IEEE, 22–31.
  - [32] NVIDIA. 2022. *NVIDIA GPU Memory Error Management*. <https://docs.nvidia.com/deploy/pdf/a100-gpu-mem-error-mgmt.pdf>
  - [33] NVIDIA. 2023. *NVIDIA Data Center GPU Driver version 525.105.17 (Linux) / 528.89 (Windows)*. [https://docs.nvidia.com/datacenter/tesla/pdf/NVIDIA\\_Data\\_Center\\_GPU\\_Driver\\_Release\\_Notes\\_525\\_v3.0.pdf](https://docs.nvidia.com/datacenter/tesla/pdf/NVIDIA_Data_Center_GPU_Driver_Release_Notes_525_v3.0.pdf)
  - [34] NVIDIA. 2024. *GPU Deployment and Management*. [https://docs.nvidia.com/deploy/pdf/XID\\_Errors.pdf](https://docs.nvidia.com/deploy/pdf/XID_Errors.pdf)
  - [35] Official, AWS. 2023. *Troubleshoot xid errors in Nvidia GPU-accelerated instances*. <https://repost.aws/knowledge-center/ec2-linux-troubleshoot-xid-errors>
  - [36] Vladyslav Oles, Anna Schmieding, George Ostrouchov, Woong Shin, Evgenia Smirni, and Christian Engelmann. 2024. Understanding GPU Memory Corruption at Extreme Scale: The Summit Case Study. In *Proceedings of the 38th ACM International Conference on Supercomputing*. 188–200.
  - [37] George Ostrouchov, Don Maxwell, Rizwan A Ashraf, Christian Engelmann, Mallikarjun Shankar, and James H Rogers. 2020. GPU lifetimes on Titan supercomputer: Survival analysis and reliability. In *SC20: International Conference for High Performance Computing, Networking, Storage and Analysis*. IEEE, 1–14.
  - [38] Jon Perez-Cerrolaza, Jaume Abella, Leonidas Kosmidis, Alejandro J Calderon, Francisco Cazorla, and Jose Luis Flores. 2022. GPU devices for safety-critical systems: A survey. *Comput. Surveys* 55, 7 (2022), 1–37.
  - [39] James C Phillips, Rosemary Braun, Wei Wang, James Gumbart, Emad Tajkhorshid, Elizabeth Villa, Christophe Chipot, Robert D Skeel, Laxmikant Kale, and Klaus Schulten. 2005. Scalable molecular dynamics with NAMD. *Journal of computational chemistry* 26, 16 (2005), 1781–1802.
  - [40] PyTorch Contributors. 2017. *PyTorch Issue #1137: How to Handle Corrupted Data in Dataloader*. <https://github.com/pytorch/pytorch/issues/1137> Accessed: 2024-11-26.
  - [41] PyTorch Contributors. 2018. *Discussion: How to Handle Exception in DistributedDataParallel*. <https://discuss.pytorch.org/t/how-to-handle-exception-in-distributeddataparallel/42026> Accessed: 2024-11-26.
  - [42] PyTorch Lightning Contributors. 2021. *PyTorch Lightning Discussion: Handling Exceptions in Forward Pass*. <https://github.com/Lightning-AI/pytorch-lightning/discussions/15188> Accessed: 2024-11-26.
  - [43] Paolo Rech, Laécio Lima Pilla, Philippe Olivier Alexandre Navaux, and Luigi Carro. 2014. Impact of GPUs parallelism management on safety-critical and HPC applications reliability. In *2014 44th Annual IEEE/IFIP International Conference on Dependable Systems and Networks*. IEEE, 455–466.
  - [44] G.P. Saggese, A. Vetteth, Z. Kalbarczyk, and Ravishankar Iyer. 2005. Micro-processor sensitivity to failures: control vs. execution and combinational vs. sequential logic. In *2005 International Conference on Dependable Systems and Networks (DSN'05)*. 760–769. <https://doi.org/10.1109/DSN.2005.63>
  - [45] Dimitris Sartzetakis, George Papadimitriou, and Dimitris Gizopoulos. 2022. gpufi-4: A microarchitecture-level framework for assessing the cross-layer resilience of nvidia gpus. In *2022 IEEE International Symposium on Performance Analysis of Systems and Software (ISPASS)*. IEEE, 35–45.
  - [46] Gabin Schieffer, Jacob Wahlgren, Jie Ren, Jennifer Faj, and Ivy Peng. 2024. Harnessing integrated cpu-gpu system memory for hpc: a first look into grace hopper. In *Proceedings of the 53rd International Conference on Parallel Processing*. 199–209.
  - [47] Deval Shah, Zi Yu Xue, Karthik Pattabiraman, and Tor M Aamodt. 2024. Characterizing and Improving Resilience of Accelerators to Memory Errors in Autonomous Robots. *ACM Transactions on Cyber-Physical Systems* 8, 3 (2024), 1–33.
  - [48] Gilad Shainer, Tong Liu, John Michalakes, Jacob Liberman, Jeff Layton, Onur Celebioglu, Scot A Schultz, Joshua Mora, and David Cownie. 2009. Weather research and forecast (WRF) model performance and profiling analysis on advanced multi-core HPC clusters. *10th LCI ICHPC* (2009).
  - [49] David Skinner and William Kramer. 2005. Understanding the causes of performance variability in HPC workloads. In *IEEE International. 2005 Proceedings of the IEEE Workload Characterization Symposium, 2005*. IEEE, 137–149.
  - [50] Veeras Sridharan, Nathan DeBardeleben, Sean Blanchard, Kurt B. Ferreira, Jon Stearley, John Shalf, and Sudhanva Gurumurthi. 2015. Memory Errors in Modern Systems: The Good, The Bad, and The Ugly. *SIGPLAN Not.* 50, 4 (March 2015), 297–310. <https://doi.org/10.1145/2775054.2694348>
  - [51] Gemini Team, Rohan Anil, Sebastian Borgeaud, Jean-Baptiste Alayrac, Jiahui Yu, Radu Soricut, Johan Schalkwyk, Andrew M Dai, Anja Hauth, Katie Millican, et al. 2023. Gemini: a family of highly capable multimodal models. *arXiv preprint arXiv:2312.11805* (2023).
  - [52] Devesh Tiwari, Saurabh Gupta, George Gallarno, Jim Rogers, and Don Maxwell. 2015. Reliability lessons learned from gpu experience with the titan supercomputer at oak ridge leadership computing facility. In *Proceedings of the international conference for high performance computing, networking, storage and analysis*. 1–12.
  - [53] Devesh Tiwari, Saurabh Gupta, James Rogers, Don Maxwell, Paolo Rech, Sudharshan Vazhkudai, Daniel Oliveira, Dave Londo, Nathan DeBardeleben, Philippe Navaux, et al. 2015. Understanding GPU errors on large-scale HPC systems and the implications for system design and operation. In *2015 IEEE 21st International Symposium on High Performance Computer Architecture (HPCA)*. IEEE, 331–342.
  - [54] Hugo Touvron, Thibaut Lavril, Gautier Izacard, Xavier Martinet, Marie-Anne Lachaux, Timothée Lacroix, Baptiste Rozière, Naman Goyal, Eric Hambro, Faisal Azhar, et al. 2023. Llama: Open and efficient foundation language models. *arXiv preprint arXiv:2302.13971* (2023).
  - [55] Alessandro Vallerio, Sotiris Tselonis, Dimitris Gizopoulos, and Stefano Di Carlo. 2018. Multi-faceted microarchitecture level reliability characterization for nvidia and amd gpus. In *2018 IEEE 36th VLSI Test Symposium (VTS)*. IEEE, 1–6.
  - [56] Borui Wan, Mingji Han, Yiyao Sheng, Yanghua Peng, Haibin Lin, Mofan Zhang, Zhichao Lai, Menghan Yu, Junda Zhang, Zuquan Song, et al. 2024. ByteCheckpoint: A Unified Checkpointing System for Large Foundation Model Development. *arXiv preprint arXiv:2407.20143* (2024).
  - [57] Long Wang, Karthik Pattabiraman, Zbigniew Kalbarczyk, Ravishankar K Iyer, Lawrence Votta, Christopher Vick, and Alan Wood. 2005. Modeling coordinated checkpointing for large-scale supercomputers. In *2005 International Conference on Dependable Systems and Networks (DSN'05)*. IEEE, 812–821.
  - [58] Xiaohui Wei, Hengshan Yue, Shang Gao, Lina Li, Ruyi Zhang, and Jingweijia Tan. 2020. G-SEAP: Analyzing and characterizing soft-error aware approximation in GPGPUs. *Future Generation Computer Systems* 109 (2020), 262–274.
  - [59] Qizhen Weng, Wencong Xiao, Yinghao Yu, Wei Wang, Cheng Wang, Jian He, Yong Li, Liping Zhang, Wei Lin, and Yu Ding. 2022. MLaaS in the Wild: Workload Analysis and Scheduling in Large-Scale Heterogeneous GPU Clusters. In *19th USENIX Symposium on Networked Systems Design and Implementation (NSDI 22)*. USENIX Association, Renton, WA, 945–960. <https://www.usenix.org/conference/nsdi22/presentation/weng>
  - [60] Lishan Yang, George Papadimitriou, Dimitris Sartzetakis, Adwait Jog, Evgenia Smirni, and Dimitris Gizopoulos. 2024. GPU Reliability Assessment: Insights Across the Abstraction Layers. In *2024 IEEE International Conference on Cluster Computing (CLUSTER)*. IEEE, 1–13.
  - [61] Andy B. Yoo, Morris A. Jette, and Mark Grondona. 2003. SLURM: Simple Linux Utility for Resource Management. In *Job Scheduling Strategies for Parallel Processing*. Dror Feitelson, Larry Rudolph, and Uwe Schwiegelshohn (Eds.). Springer Berlin Heidelberg, Berlin, Heidelberg, 44–60.